Journal of Materials Chemistry B

PAPER

Cite this: J. Mater. Chem. B, 2015, 3, 4723

Positive charge of "sticky" peptides and proteins impedes release from negatively charged PLGA matrices†

Stephen C. Balmert,‡[ab] Andrew C. Zmolek,‡[c] Andrew J. Glowacki,[bc] Timothy D. Knab,[bc] Sam N. Rothstein,[bc] Joseph M. Wokpetah,[c] Morgan V. Fedorchak[bcd] and Steven R. Little*[abce]

Received 20th March 2015,
Accepted 20th May 2015

DOI: 10.1039/c5tb00515a

www.rsc.org/MaterialsB

The influence of electrostatic interactions and/or acylation on release of charged ("sticky") agents from biodegradable polymer matrices was systematically characterized. We hypothesized that release of peptides with positive charge would be hindered from negatively charged poly(lactic-*co*-glycolic acid) (PLGA) microparticles. Thus, we investigated release of peptides with different degrees of positive charge from several PLGA microparticle formulations, with different molecular weights and/or end groups (acid- or ester-terminated). Indeed, release studies revealed distinct inverse correlations between the amount of positive charge on peptides and their release rates from each PLGA microparticle formulation. Furthermore, we examined the case of peptides with net charge that changes from negative to positive within the pH range observed in degrading microparticles. These charge changing peptides displayed counterintuitive release kinetics, initially releasing faster from slower degrading (less acidic) microparticles, and releasing slower from the faster degrading (more acidic) microparticles. Importantly, trends between agent charge and release rates for model peptides also translated to larger, therapeutically relevant proteins and oligonucleotides. The results of these studies may improve future design of controlled release systems for numerous therapeutic biomolecules exhibiting positive charge, ultimately reducing time-consuming and costly trial and error iterations of such formulations.

Introduction

The global market for peptide and protein drugs is projected to reach $179 billion by 2018,[1] and combined sales of 25 FDA-approved peptide therapeutics (<50 amino acids) exceeded $14 billion in 2011.[2] Still, the overwhelming potential of therapeutic peptides and proteins has been limited, in part, by short half-life (minutes to hours) and insufficient bioavailability when administered orally. As a result, frequent injections may be needed to deliver sufficient levels of bioactive peptides or proteins, which could exacerbate issues with patient compliance. Controlled release systems have the potential to dramatically prolong bioavailability of rapidly cleared drugs (*e.g.* peptides and proteins) and maintain therapeutic levels for weeks to months with less frequent dosing. In turn, improved patient compliance and therapeutic efficacy could save the U.S. healthcare system upwards of $100 billion each year[3]—more than the total annual direct costs for treating cancer.[4]

A major challenge for developing controlled release formulations is tuning release kinetics to achieve the desired dosing schedule for a given therapeutic agent. As one of the most common types of controlled release systems, biodegradable polymer matrices are often fabricated as microspheres or microparticles (MPs) given the ease of loading and minimally invasive implantation through a needle and syringe. These matrices can be fabricated to be practically any size using many common polymers that are commercially available in a variety of molecular weights. In the past twenty-five years, numerous studies have identified key physical properties of such delivery systems that determine their release behavior (reviewed in ref. 5 and 6). Mathematical models developed by our group and others have enabled predictions of release kinetics based on such factors as matrix geometry, polymer chemistry, and drug/agent molecular weight.[7,8] Although drug–polymer interactions have been cited as factors affecting release from poly(lactic-*co*-glycolic acid) (PLGA) MPs,[9] the effects of such interactions on release kinetics have not yet been extensively studied or characterized.

[a] Department of Bioengineering, University of Pittsburgh, 940 Benedum Hall, 3700 O'Hara Street, Pittsburgh, PA, USA. E-mail: srlittle@pitt.edu; Fax: +1 412-624-9639; Tel: +1 412-624-9614
[b] McGowan Institute for Regenerative Medicine, University of Pittsburgh, PA, USA
[c] Department of Chemical Engineering, University of Pittsburgh, PA, USA
[d] Department of Ophthalmology, University of Pittsburgh, PA, USA
[e] Department of Immunology, University of Pittsburgh, PA, USA

† Electronic supplementary information (ESI) available. See DOI: 10.1039/c5tb00515a

‡ S.C.B. and A.C.Z. contributed equally to this work

For the past few decades, synthetic biodegradable polymers, such as polyesters (*e.g.* PLGA), poly(*ortho* esters), and polyanhydrides, have been used extensively for drug delivery. PLGA is an especially attractive biomaterial for controlled release systems because of its tunable degradation rate, proven biocompatibility, and outstanding history of FDA approval.[10] This includes at least nine MP drug delivery formulations currently on the market.[11] Importantly, progressive hydrolytic degradation of polyesters, poly(*ortho* esters), and polyanhydrides produces increasingly shorter polymer chains with carboxylic acid end groups. In aqueous solution, these carboxylic acid groups dissociate into carboxylate anions, conferring negative charge on the polymers. As a result of this negative charge, which increases over time due to polymer degradation, ionic interactions between PLGA matrices and positively charged (cationic) peptides have been observed.[12–14] A recent study even demonstrated that cationic peptides could be adsorbed to the surface of low molecular weight PLGA MPs or thin films for extended delivery *via* subsequent desorption.[15] Additionally, several groups have demonstrated that positively charged peptides can become acylated in PLGA matrices.[16–18] Acylation reactions between nucleophilic (high pK_a) primary amines in peptides (*e.g.* lysine residues and N-termini) and PLGA ester bonds form new covalent bonds between peptides and PLGA oligomers, resulting in peptide–PLGA adducts.[16] Peptide sorption to PLGA (as by electrostatic interactions) is also believed to be a precursor to peptide acylation.[12] Since many therapeutic proteins, peptides, and small molecule drugs contain positively charged functional groups, better characterization and understanding of the effects of electrostatic interactions and/or acylation reactions between these agents and negatively charged polymers on release kinetics could improve tools for predicting release and designing controlled release systems.

We hypothesized that positively charged peptides (and larger biomolecules) would exhibit a variable degree of "stickiness" to a polymer matrix with negative charge, thereby reducing their diffusion through the polymer matrix and impeding release from MPs. We further hypothesized that greater positive charge on a peptide would lead to slower release, due to electrostatic interactions and/or acylation. Herein, we demonstrate that release of peptides from PLGA MPs is, in fact, inversely correlated with the peptides' net positive charge, which may increase with a decrease in pH of the surrounding microenvironment. We also show that pH of the intraparticle microenvironment, which decreases over time, depends greatly on PLGA initial molecular weight and end group chemistry. Notably, in some cases, peptide charge may even switch from negative to positive with the drop in pH in degrading PLGA MPs. Together, these observations allow us to explain previously unintuitive trends in early release behavior for some peptides that release faster from slower degrading (higher initial intraparticle pH) polymers. Finally, we show that trends identified for charged peptides extend to larger biomolecules, suggesting the results of these studies are relevant to rationale design of controlled release systems for delivery of a broad range of therapeutic proteins, growth factors, cytokines, and oligonucleotides.

Experimental

Materials

Four poly(D,L-lactic-*co*-glycolic acid) (PLGA) polymers, with 50 : 50 lactide : glycolide composition and different molecular weights and end groups, were purchased from Sigma Aldrich (St. Louis, MO; supplier of Evonik RESOMER RG502H, RG504H, and RG502 polymers) and Lakeshore Biomaterials (Birmingham, AL; supplier of Evonik 5050 DLG1A). Poly(vinyl alcohol) (PVA, 98 mol% hydrolyzed, M_w = 25 000 g mol^{-1}) was purchased from PolySciences (Warrington, PA). Seven peptides, fluorescently labeled with 5-carboxytetramethyl-rhodamine (5-TAMRA), or HiLyte Fluor 488 (HF488), were obtained from AnaSpec (Fremont, CA) (see Table 1). Recombinant murine CCL22 and CCL21 were obtained from R&D Systems (Minneapolis, MN). Ovalbumin labeled with Texas Red was obtained from Life Technologies (Grand Island, NY). STAT3 cyclic decoy oligodeoxynucleotide (ODN)[19] was generously provided by Malabika Sen and Jennifer Grandis (University of Pittsburgh).

Microparticle (MP) fabrication

Microparticles (MPs) containing one of the eight fluorescently labeled peptides, rmCCL22, or rmCCL21, were fabricated using a double emulsion-evaporation technique, as described previously.[20,21] Briefly, MPs were prepared by mixing 200 μL of an aqueous solution containing the respective agent (125 μg of fluorescently labeled peptide, 5 μg of rmCCL22 or rmCCL21, 200 μg of ovalbumin, or 1 mg of STAT3 cyclic decoy ODN) with 200 mg of 50 : 50 PLGA (DLG1A, RG502H, RG502, or RG504H) dissolved in 4 mL of dichloromethane. This mixture was sonicated (Vibra-Cell VC750; Sonics, Newton, CT) at 25% amplitude for 10 s to form the first emulsion (water-in-oil, w/o), and then poured into a 2% PVA solution (60 mL) being homogenized

Table 1 Peptides Used for Release Studies

Peptide	Label & amino acid sequence	ID[a]	Associated figures
CDK7tide	5-TAMRA-YSPTSPSYSPTSPSYSPTSPS	+0.0	1, 2, 3 and 5D
Erktide	5-TAMRA-IPTTPITTTYFFFK	+0.5	2, 3 and 5D
CHK1tide	5-TAMRA-ALKLVRYPSFVITAK	+1.4	2, 3 and 5D
Neurogranin 28–43	5-TAMRA-AAKIQASFRGHMARKK	+2.7	2, 3 and 5D
PKCε peptide substrate	5-TAMRA-ERMRPRKRQGSVRRRV	+3.1	2, 3 and 5D
Casein kinase 1 substrate	5-TAMRA-RRKDLHDDEEDEAMSITA	CK1sub	5
Beta-amyloid 1–17	HF488-DAEFRHDSGYEVHHQKL	BA17	5D and S2 (ESI)

[a] Identifier used in figures: net charge per mass (kDa^{-1}) at pH 4 for pH-independent peptides, or abbreviated name for pH-dependent peptides.

(L4RT-A; Silverson, East Longmeadow, MA) at 3000 rpm. Following 1 min of homogenization, the resulting double emulsion (w/o/w) was added to a 1% PVA solution (80 mL) and stirred for 3 h to allow the dichloromethane to evaporate. Freshly formed MPs were centrifuged (300 g for 5 min at 4 °C) and washed 4 times with deionized water (DIW). The MPs were then re-suspended in DIW (5 mL), flash-frozen with liquid nitrogen, and lyophilized (Benchtop 2K Freeze Dryer; VirTis, Gardiner, NY; operating at 80 mTorr).

Microparticle characterization and release assays

Scanning electron micrographs of microparticles (MPs) were obtained using a scanning electron microscope (JSM-6330F; JEOL, Peabody, MA). Size distributions of MPs were determined using volume impedance measurements on a Beckman Coulter Counter (Multisizer-3; Beckman Coulter, Brea, CA). *In vitro* release behavior for all MP formulations was characterized by incubating 10 mg of MPs in 1 mL of phosphate buffered saline (PBS) on a roto-shaker at 37 °C. At regular time intervals, MP suspensions were centrifuged, the supernatants were removed, and the MPs were re-suspended in fresh PBS. Supernatant concentrations of released agents were quantified by fluorescence spectrophotometry (SpectraMax M5; Molecular Devices, Sunnyvale, CA) for fluorescently labeled peptides and ovalbumin, enzyme-linked immunosorbant assay (ELISA; R&D Systems) for CCL22 and CCL21, and Quant-iT dsDNA assay (Life Technologies) for the STAT3 cyclic decoy ODN. Release profiles generated from measured concentrations of peptide, protein, or ODN were normalized to total amounts encapsulated. All release assay experiments were performed in triplicate, and data represent means with standard deviation error bars.

Intraparticle pH measurements

As described previously,[22,23] hydrogen ion concentration of dissolved PLGA MPs was measured and converted to average pH of the intraparticle microenvironment, based on the total aqueous volume of hydrated MPs. Briefly, 10 mg of MPs were incubated in 1 mL of PBS (pH 7.4) on a roto-shaker at 37 °C. At predetermined time points, the MP suspensions were centrifuged, and the supernatant was removed. The remaining MPs and associated aqueous microenvironment were then dissolved in 800 μL of acetonitrile (ACN) by vigorous vortexing. Tubes were centrifuged a second time to remove any undissolved PLGA, and 800 μL of this ACN + PBS + PLGA solution was added to 200 μL of deionized water (DIW) prior to pH measurements with an InLab Routine Pro pH probe (Mettler Toledo, Columbus, OH). To determine the pH of the MPs and aqueous microenvironment, we obtained a correlation between the pH of lactic acid monomers in PBS and lactic acid monomers in a mixture of PBS, ACN, and DIW (comparable to the dissolved PLGA MPs). Based on the measured pH values and total aqueous volume of the hydrated MPs, average intraparticle pH could be estimated. Supernatant pH was also measured.

Biomolecule net charge predictions

Net charge of peptides and proteins (Z), which is based on the protonation state of amino acid side groups and the C- and N-termini, was calculated as a function of pH, according to:

$$Z = \sum_i N_i \frac{10^{pK_{a_i}}}{10^{pH} + 10^{pK_{a_i}}} - \sum_j N_j \frac{10^{pK_{a_j}}}{10^{pH} + 10^{pK_{a_j}}} \quad (1)$$

where N_i and pK_{a_i} represent the number and pK_a values of the N-terminus (pK_a = 9.69) and side chains of cationic amino acid residues: arginine (12.48), lysine (10.53), and histidine (6.00). N_j and pK_{a_j} represent the number and pK_a values of the C-terminus (2.34) and side chains of anionic residues: aspartic acid (3.86), glutamic acid (4.25), cysteine (8.33), and tyrosine (10.07). Previously published pK_a values were used.[24] As noted in the figures, charge was normalized to the total mass of the peptide or protein. To determine peptide charge as a function of time, we input interpolations of measured intraparticle pH (*i.e.* pH = f(time)) into eqn (1) (charge = f(pH)). The interpolations were generated using the piecewise cubic Hermite interpolating polynomial (PCHIP) function in MATLAB (v7.12, The MathWorks, Inc., Natick, MA). Charge predictions for the cyclic oligonucleotide were calculated with the Marvin v14.8 ''protonation'' plug-in (ChemAxon LLC, Cambridge, MA).

Results

Microparticle (MP) characterization

All MPs containing peptides were prepared under similar conditions using three uncapped (–COOH acid-terminated) 50 : 50 PLGA polymers with different average initial molecular weights (7, 15, and 43 kDa), and a fourth ester-capped (–$COOCH_3$ terminated) 50 : 50 PLGA (15 kDa). Representative scanning electron micrographs (Fig. S1, ESI†) show spherical MPs with similar surface morphology, as observed for all formulations. Volume-averaged size distributions of MPs, measured with a Beckman Coulter Counter, are relatively consistent between batches, with mean diameters of 19.0 ± 3.4 μm (see Table S1 for size distributions for each formulation, ESI†). Total peptide loading was also consistent, with an average encapsulation efficiency of 78 ± 14 percent across all formulations. Total peptide loading and encapsulation efficiencies for each individual formulation can be found in supplemental Tables S2 and S3 (ESI†).

Release kinetics for an uncharged peptide depend on PLGA molecular weight and degradation rate

To establish a baseline for peptide release behavior with minimal electrostatic interactions and acylation reactions between the peptide and polymer matrix, a fluorescently labeled peptide with an amino acid sequence that yielded net neutral charge across a range of pH values was used. This peptide also lacked primary amine groups, which are common targets of acylation (*i.e.* no lysine residues, and N-terminus capped by 5-TAMRA fluorophore). This uncharged hydrophilic peptide was encapsulated in MPs comprised of acid-terminated 50 : 50 PLGA with three different initial molecular weights (7 kDa, 15 kDa, and 43 kDa), and an ester-terminated (capped) 15 kDa PLGA (''15 kDa-E''). Ester-capped PLGA initially lacks carboxylic acid end groups, is more

hydrophobic, and thus degrades more slowly.[25] *In vitro* release assays for each formulation demonstrated a substantial effect of polymer molecular weight on release kinetics (Fig. 1). For the lowest molecular weight (7 kDa) PLGA MPs, release appeared to follow first-order kinetics with no initial delay in release, since the low molecular weight regions of the polymer matrix were already sufficiently permeable to the encapsulated peptide at the start of incubation. First-order release kinetics of the neutral peptide were progressively delayed with increasing PLGA molecular weight, resulting in initial lag phases of approximately 10 and 20 days for the 15 and 43 kDa PLGA, respectively. Due to less mobile higher molecular weight polymer chains,[7] these matrices were initially less permeable to the encapsulated peptide. Therefore, the PLGA polymers degraded with minimal release (lag phase) until regions with sufficiently low molecular weight (permeable to the peptide) formed and bulk release could begin.[7] We also observed a substantial increase in lag phase duration and decrease in the rate of subsequent release for the slower degrading ester-capped 15 kDa PLGA. Complete release of the neutral peptide occurred within 13, 37, 46, and 58 days of incubation for uncapped 7, 15, and 43 kDa PLGA and ester-capped 15 kDa PLGA, respectively (Fig. 1). These results indicate that with minimal electrostatic interactions and/or acylation reactions between a peptide and polymer matrix, polymer molecular weight and end-group chemistry control release kinetics, presumably by influencing the rate of matrix erosion and formation of interconnected porous networks through which encapsulated peptide can egress (Fig. 2A, top).[8]

Positive peptide charge dramatically impedes release, and greater charge corresponds with slower release

For positively charged peptides, we hypothesized that electrostatic interactions and/or acylation reactions with a negatively charged polymer matrix would essentially restrict diffusion of the peptides through the degrading matrix and impede release from MPs (Fig. 2A, bottom). We further hypothesized that greater positive charge on a peptide would correspond to slower release.

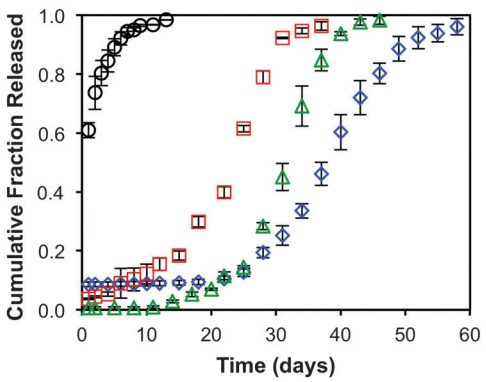

Fig. 1 Release kinetics for a neutrally charged peptide depend on PLGA initial molecular weight and end-group chemistry. Comparative *in vitro* release profiles for a 2.6 kDa peptide with net neutral charge, encapsulated in MPs with different PLGA molecular weights and end groups: 7 kDa (circles), 15 kDa (squares), 43 kDa (triangles), and ester-capped 15 kDa (diamonds).

In order to test the effects of peptide charge on release kinetics, we identified four fluorescently labeled peptides with positive net charges that were consistent across a range of pH values (Fig. 2B). These hydrophilic peptides also had similar molecular weights (2.1–2.6 kDa) to that of the neutral peptide (2.6 kDa), to eliminate any confounding effects of peptide size on release.[7] These peptides were encapsulated in microparticles comprised of each of the four aforementioned PLGA polymers, and *in vitro* release assays were conducted, as for the neutral peptide.

Compared to the neutral peptide, positively charged peptides released more slowly from all PLGA polymers (Fig. 2C–F). For the peptide with the greatest net positive charge per mass ($+3.1\ kDa^{-1}$), release was most significantly impeded. In fact, less than 20 percent of the encapsulated cationic ($+3.1\ kDa^{-1}$) peptide was released by the time at which MPs had degraded sufficiently to release nearly 100 percent of the neutral peptide. For each formulation, nearly 100 percent of the total peptide encapsulated was eventually detected; however, for comparison, release profiles graphed in Fig. 2 were cut off when the neutral peptide had completely released. As shown in Fig. 1, complete release of the neutral peptide ranged from approximately two weeks for the 7 kDa PLGA to more than 8 weeks for the ester-capped 15 kDa PLGA MPs. Notably, we observed inverse correlations between peptide charge and release rate for each polymer formulation (summarized in Fig. 3). These trends are especially consistent for each of the uncapped PLGA polymers; however, release from the ester-capped PLGA appears to be somewhat less dependent on peptide charge. This may be due to the fact that with minimal electrostatic interactions or acylation, the maximum rate of release from the slower degrading ester-capped PLGA is less than that for the uncapped polymers (3.8% *vs.* 6.6–6.9% of total peptide encapsulated per day). Counter to the trends described above, the $+0.5\ kDa^{-1}$ and $+\ 1.4\ kDa^{-1}$ peptides released slightly faster than the neutral peptide from 43 kDa and/or ester-capped 15 kDa PLGA MPs, during days 3–9 (Fig. 2E and F). These minor anomalies may be attributed to a combination of factors, including slight differences in particle size, peptide size, peptide loading, or peptide distribution within the MPs. Additionally, since the neutral peptide is somewhat less hydrophilic than the positively charged peptides, it may exhibit greater hydrophobic interactions with the more hydrophobic (higher molecular weight or ester-capped) PLGA MPs. Overall, the results of these release studies demonstrate that the amount of positive charge on peptides can influence their release kinetics dramatically, regardless of polymer formulation, and greater peptide charge contributes to slower release.

Intraparticle pH decreases with time and depends on PLGA initial molecular weight and end groups

Previous studies have noted that pH within degrading PLGA MPs is acidic and dynamic, decreasing over time as more carboxylic acid end groups are produced by progressive hydrolysis of the PLGA backbone;[23,26,27] however, the effects of polymer initial molecular weight and end-group chemistry on intraparticle pH have not been examined. Changes in pH during particle degradation, or differences

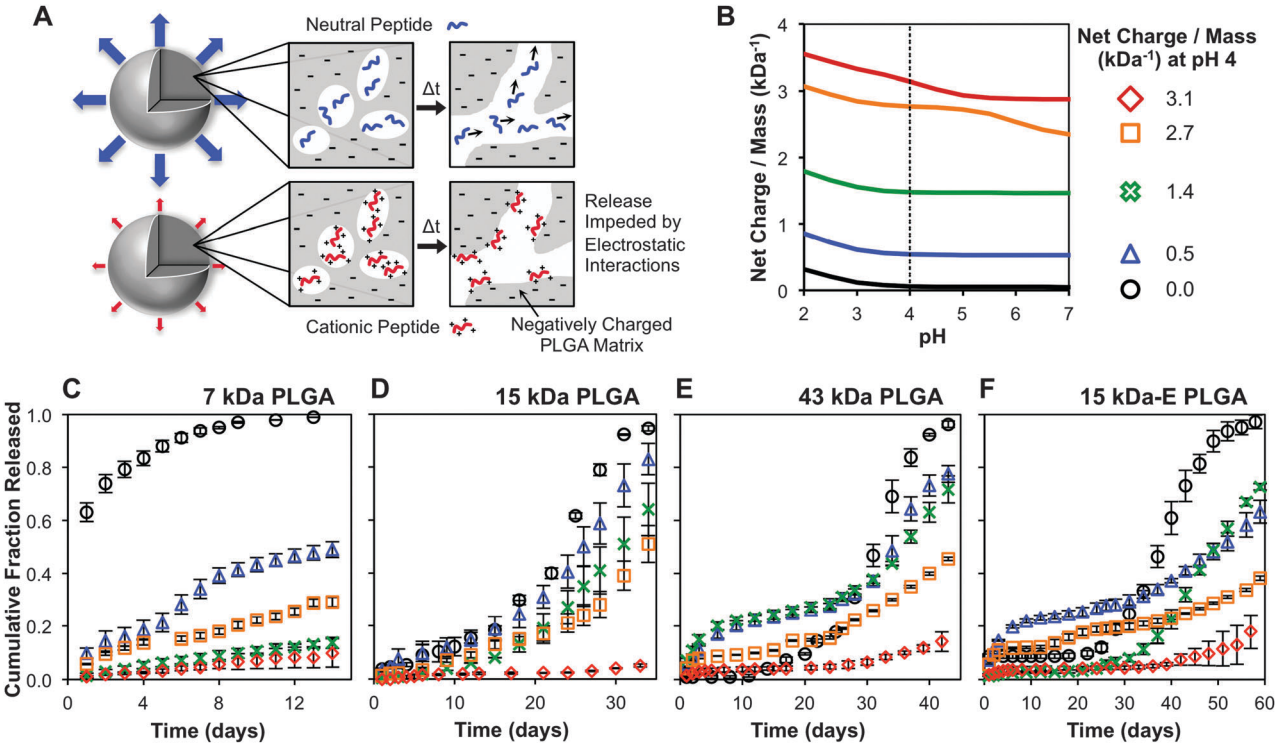

Fig. 2 Greater net positive charge on a peptide corresponds with a reduction in release kinetics from negatively charged PLGA matrices. (A) Proposed mechanism by which peptide charge influences release kinetics. Polymer degradation and matrix erosion over time form increasingly interconnected pores. Unlike neutral peptides, cationic peptides may stick to the polymer matrix *via* electrostatic interactions and/or acylation, thereby impeding release. (B) Calculated net charge per mass, as a function of pH, for five peptides with similar molecular weights (2.3 ± 0.2 kDa). (C–F) *In vitro* release kinetics for those five peptides, encapsulated in MPs with different PLGA molecular weights and end-groups: (C) 7 kDa, (D) 15 kDa, (E) 43 kDa, (F) ester-capped 15 kDa-E. Release profiles are truncated at time points corresponding to complete release for the neutral peptide (black circles).

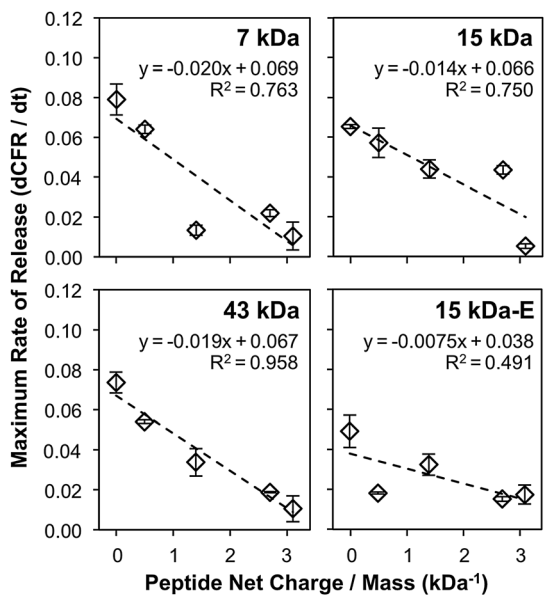

Fig. 3 Release rates of peptides from PLGA MPs are inversely related to the peptides' net positive charge. Data represent maximum release rates for each MP formulation in Fig. 2, grouped by polymer molecular weight. The maximum rate of release (*i.e.* the maximum of d(Cumulative Fraction Released)/d*t*, or dCFR/d*t*) typically follows the lag phase, and any initial burst is not considered. dCFR/d*t* = 0.1 corresponds to a rate of 10 percent of total release per day.

in intraparticle pH among polymer formulations, would have nominal effects on net charge of the aforementioned five peptides (Fig. 2B) since they are composed of uncharged and basic residues (positive at pH < 7). However, for peptides with a greater frequency of both acidic and basic residues, net charge would vary greatly depending on the pH of the surrounding microenvironment (for pH < 7), and could even switch from negative to positive as pH drops. More acidic intraparticle pH could also catalyze peptide acylation reactions.[16] In order to determine the dynamic charge of such peptides, we first measured bulk intraparticle pH of four different PLGA MP formulations incubating in PBS for up to three weeks (Fig. 4A). Comparison of intraparticle pH in the different MPs illustrates the dramatic impact of PLGA initial molecular weight and end group chemistry on the evolution of intraparticle pH. For MPs made of higher molecular weight or ester-capped PLGA, intraparticle pH was higher initially and decreased more gradually. Average initial intraparticle pH (after 1 hour of incubation in PBS) was 6.0 and 5.9 for the 43 kDa and ester-capped 15 kDa PLGA MPs, compared to 4.5 and 3.6 for the lower molecular weight, uncapped polymers (7 and 15 kDa). Intraparticle pH of the 7 kDa PLGA MPs dropped considerably to 3.3 by day 3 and gradually decreased to a minimum of 2.2 by day 12. The 15 kDa PLGA MPs exhibited a similar decrease in pH to a minimum of 2.4 by day 18. In contrast, MPs comprised of 43 kDa or ester-capped 15 kDa PLGA polymers had

more moderate drops in intraparticle pH to 3.2 or 3.4 by day 21 (Fig. 4A). Lower intraparticle pH for 7 and 15 kDa PLGA MPs was accompanied by marked decreases in supernatant pH to 3.5 (7 kDa, day 12) and 4.1 (15 kDa, day 18) (Fig. 4B). In contrast, supernatant pH for the 43 kDa and ester-capped 15 kDa PLGA MPs never dropped below 5.7 or 6.4, respectively, after 21 days (Fig. 4B). Collectively, the intraparticle pH measurements suggest that agents encapsulated in PLGA MPs with different polymer chemistry (molecular weight and end-groups) would experience microenvironments with different pH.

Early release behavior is influenced by initial peptide charge, and depends on initial intraparticle pH

To investigate the effects of pH-dependent peptide charge on release kinetics, we identified a fluorescently labeled peptide (“CK1sub”) with a low isoelectric point (pI 4.16) that falls within the range of intraparticle pH observed in degrading PLGA MPs (Fig. 4A). Net charge of this peptide—and others that contain abundant acidic (Asp, Glu) and basic (Arg, Lys, His) amino acid residues—depends greatly on pH, and transitions from negative to positive as pH drops below its isoelectric point (Fig. 5A). Based on intraparticle pH measurements (Fig. 4A) and CK1sub’s pH-dependent charge (Fig. 5A), we were able to estimate its net charge over time in the various polymer formulations. Notably, the lower initial intraparticle pH for uncapped 15 kDa PLGA MPs, relative to ester-capped 15 kDa PLGA MPs (Fig. 4A), contributed to striking differences in peptide charge during the initial week of release (Fig. 5B). Specifically, initial net charge of the CK1sub peptide was predicted to be positive in uncapped PLGA (Fig. 5B, red), due to the lower initial intraparticle pH, but negative in ester-capped PLGA (Fig. 5B, blue), due to the higher initial pH. Accordingly, we hypothesized that CK1sub would exhibit greater early release from ester-capped PLGA than from uncapped PLGA, due to fewer electrostatic interactions with the polymer matrix. As predicted, release profiles indicated accelerated early release kinetics and greater initial burst from ester-capped PLGA when compared to uncapped PLGA (Fig. 5C). This result was consistent with our hypothesis, but could otherwise appear to be counterintuitive under the expectation that the more hydrophobic, slower degrading, ester-capped polymer would produce slower release.[28] Similar results for another pH-dependent peptide (beta-amyloid “BA17”) with a low isoelectric point (pI 5.75) corroborate the trends in release we observed for CK1sub: BA17 also exhibited greater initial burst from ester-capped *vs.* uncapped PLGA (Fig. S2, ESI†).

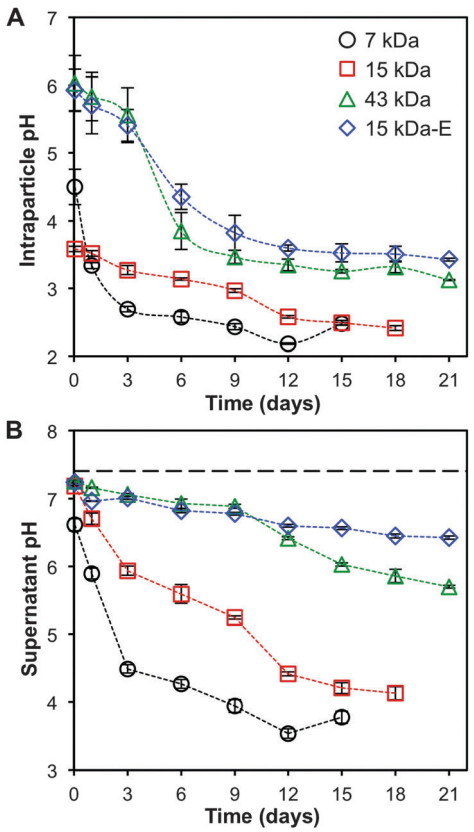

Fig. 4 Intraparticle pH and supernatant pH are dynamic and depend on PLGA initial molecular weight and degradation rate. (A) Intraparticle pH measurements for MPs made of 7 kDa (black circles), 15 kDa (red squares), 43 kDa (green triangles), or ester-capped 15 kDa-E PLGA (blue diamonds). (B) Corresponding measured supernatant pH for the microparticle formulations. Dashed line at pH 7.4 represents the pH of PBS. Data represent mean ± SD for 3–6 independent samples.

For all peptides studied (pH dependent and independent), we observed distinct inverse correlations between initial burst (fraction released within the first 24 hours) and initial peptide charge within certain PLGA matrices (Fig. 5D). When encapsulated in 7 kDa or ester-capped 15 kDa PLGA MPs, peptides with negative initial net charge (Fig. 5D, data points in grey regions) exhibited greater burst release than those with positive net charge. This suggests that initial burst of positively charged peptides is inhibited by electrostatic interactions with these polymer matrices. Since the initial intraparticle pH for uncapped 15 kDa PLGA MPs (pH 3.6, Fig. 4A) was below the isoelectric points of all peptides (see Fig. 2B, 5A, and Fig. S2A, ESI†), none of these peptides were negatively charged when encapsulated in these MPs. This includes the pH-dependent peptides (BA17 and CK1sub, identified by black arrows in Fig. 5D), which though negatively charged in the ester-capped 15 kDa PLGA MP, were positively charged in uncapped 15 kDa PLGA MPs. Consequently, minimal initial burst of all peptides from uncapped 15 kDa PLGA MPs can be attributed to electrostatic interactions with the polymer matrix. On the other hand, minimal initial burst of all peptides from 43 kDa PLGA MPs (Fig. 5D), including those with negative or neutral initial charge, suggests that peptides are retained in these MPs by physical barriers (*i.e.* a less permeable matrix). This result is consistent with previous reports that initial burst is influenced by polymer molecular weight, with less initial burst from higher molecular weight polymers.[28] In fact, for negatively charged peptides, burst release decreased with increasing polymer molecular weight, or decreasing matrix permeability (Fig. 5D, top to bottom). Specifically, initial burst of negatively charged peptides was 60–80%, 20–30%, and <10% for uncapped 7 kDa, ester-capped 15 kDa, and uncapped 43 kDa PLGA MPs, respectively (Fig. 5D). Taken together, these results suggest that burst

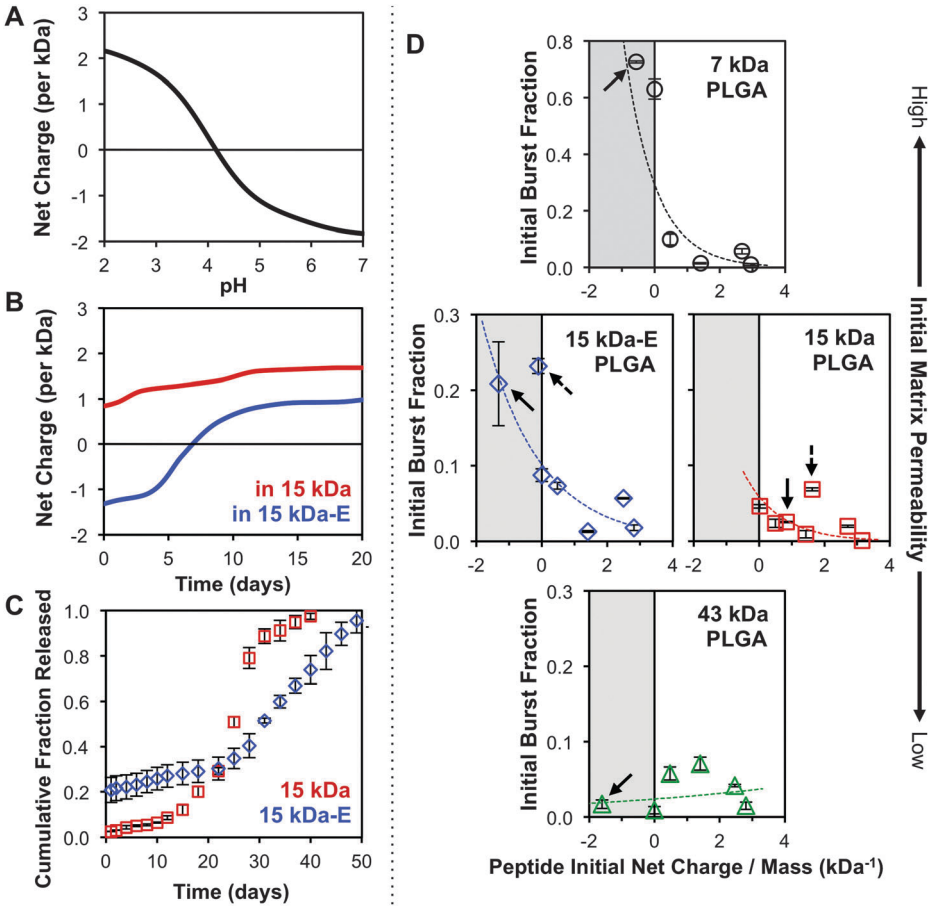

Fig. 5 For sufficiently permeable matrices, initial burst is strongly influenced by net peptide charge, which can depend on initial pH of the microenvironment in hydrated MPs. (A) Net charge as a function of pH (normalized to peptide mass) for CK1sub peptide, which has a low isoelectric point (pI < 5) and pH-dependent charge. (B) Temporally dynamic net charge estimates for CK1sub encapsulated in uncapped (red) or ester-capped (blue) 15 kDa PLGA MPs. Charge predictions are based on intraparticle pH measurements and pH-dependent peptide charge. (C) Cumulative release profiles for CK1sub encapsulated in uncapped (red squares) or ester-capped (blue diamonds) 15 kDa PLGA MPs, showing greater early release from ester-capped PLGA MPs. (D) Magnitude of initial burst (release in first 24 hours), as a fraction of total peptide encapsulated, for all controlled release formulations, including those for positively charged peptides (from Fig. 2) and pH-dependent peptides (from Fig. 5 and Fig. S2, ESI†). Each peptide's initial net charge is estimated using initial intraparticle pH measurements and the peptide's charge *vs.* pH relationship. Solid and dashed arrows identify pH-dependent CK1sub and BA17 peptides, which are positively charged in uncapped 15 kDa PLGA (red), but negatively charged in ester-capped 15 kDa PLGA (blue). Peptides in the grey regions would have minimal electrostatic interactions with the negatively charged PLGA matrix, but may be retained physically by less permeable matrices associated with higher molecular weight polymers.[15,28]

release depends on both electrostatic interactions and matrix permeability, and negatively charged peptides exhibit significantly greater initial burst than positively charged peptides, from polymer matrices with sufficient initial permeability.

Effects of positive charge on release kinetics extend to larger biomolecules with therapeutic applications

To determine whether the effects of electrostatic interactions and/or acylation reactions between positively charged agents and negatively charged PLGA MPs extend to larger biomolecules, we examined release kinetics of several therapeutically relevant proteins and oligonucleotides (8 to 43 kDa molecular weight). Specifically, we compared release kinetics of two proteins with greater positive charge density (CCL22 and CCL21) to release kinetics of two less positively charged proteins (ovalbumin and interleukin-2 (IL-2)), or an oligodeoxynucleotide (ODN; STAT3 cyclic decoy[19]) with net negative charge. For each of the five biomolecules, net charge (per mass) across a range of intraparticle pH (2 to 7) is presented in Fig. 6A. CCL21 and CCL22, with high isoelectric points (pI 10.4 and 9.7), are positively charged at any intraparticle pH. In contrast, ovalbumin and IL-2 (pI 5.0 and 4.7) have net charge that shifts from negative to neutral to positive with a drop in intraparticle pH. Even at pH 2, CCL21 and CCL22 have approximately twice the positive charge per mass as ovalbumin and IL-2 (Fig. 6A).

When encapsulated in 7 kDa PLGA MPs, positively charged CCL22 released considerably slower than neutral/negative ovalbumin (Fig. 6B), even though CCL22 (7.8 kDa) is five times smaller than ovalbumin (42.9 kDa). Similarly, when encapsulated in 15 kDa PLGA MPs, positively charged CCL21 released substantially slower than ovalbumin (Fig. 6C), again despite the fact that CCL21 (12.1 kDa) is less than a third the size of

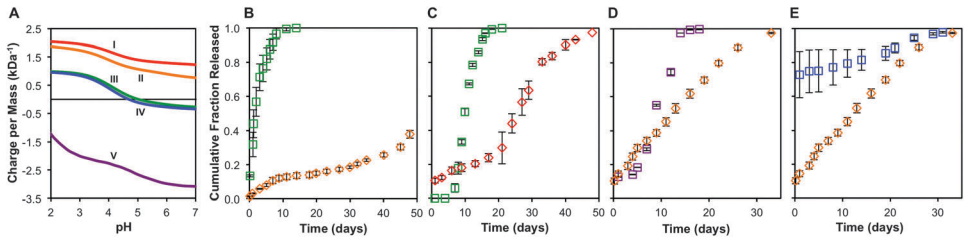

Fig. 6 Differences in net charge density on various larger biomolecules (proteins and oligonucleotides) could explain differences in release kinetics from PLGA MPs. (A) Charge density predictions as a function of pH for five larger (8–43 kDa) biomolecules. Release kinetics for: (B) ovalbumin (green squares) *vs.* CCL22 (orange diamonds) encapsulated in nonporous 7 kDa PLGA MPs, (C) ovalbumin (green squares) *vs.* CCL21 (red diamonds) encapsulated in nonporous 15 kDa PLGA MPs, (D) a STAT3 cyclic decoy oligodeoxynucleotide (ODN; violet squares) from nonporous 15 kDa PLGA MPs *vs.* CCL22 from porous 15 kDa PLGA MPs (orange diamonds), and (E) Interleukin-2 (IL-2; blue squares) *vs.* CCL22 from similarly porous 15 kDa PLGA MPs (orange diamonds). CCL22 release data in (D) and (E) adapted with permission from ref. 20. Copyright 2012, Wiley-VCH. IL-2 release data in (E) adapted with permission from ref. 21. Copyright 2012, Elsevier. Ovalbumin release data in (C) adapted with permission from ref. 44. Copyright 2014, Royal Society of Chemistry.

ovalbumin. Even in the case of initially porous MPs, which may have faster release kinetics due to greater accessibility of the encapsulated agent to the release media,[29] positive charge on an encapsulated biomolecule seems to considerably decrease the release rate. For example, release of CCL22 from porous 15 kDa PLGA MPs was prolonged relative to release of the STAT3 cyclic decoy ODN from nonporous 15 kDa PLGA MPs (Fig. 6D). Finally, release of IL-2 from porous 15 kDa PLGA MPs was substantially accelerated, relative to CCL22 released from 15 kDa porous PLGA MPs (Fig. 6E). For both particle formulations, comparable porosity was achieved by adjusting the osmolality between the inner and outer aqueous phases of the double emulsions (+30 mM ions in inner aqueous phase).[20,21] Notably, 73% of IL-2 released in an initial burst, compared to only 14% of CCL22. Taken together, these four examples suggest that charge density on larger biomolecules can also contribute to release kinetics, with slower release of more positively charged biomolecules from similar PLGA MPs.

Discussion

For agents encapsulated within a biodegradable polymer matrix, both physical barriers to diffusion (*i.e.* impermeable regions of surrounding polymer) and electrostatic or covalent interactions between the agent and matrix may contribute to sustained release kinetics. Numerous previous studies have identified key properties of polymer matrices that influence release behavior (reviewed in ref. 5 and 6), and mathematical models have been used to predict release kinetics based on such factors, which include matrix geometry, polymer chemistry, and molecular weight of the encapsulated agent.[7,8] Such parameters dictate the timeframe of matrix erosion and the extent of erosion needed for an encapsulated agent to diffuse out of the matrix, based on the molecular weight of the agent. For example, a matrix comprised of higher molecular weight and/or slower degrading PLGA generally takes longer to become sufficiently permeable for release (as in Fig. 1), and larger encapsulated agents (*e.g.* acylated peptide–PLGA adducts or fluorescently labeled peptides, relative to unlabeled native peptides) generally require formation of larger interconnected pores. Electrostatic interactions and acylation reactions between cationic therapeutic agents and negatively charged polymeric delivery systems have also been cited as factors affecting release kinetics.[9,16,17] A few studies have even shown that adsorption/desorption of certain cationic proteins or peptides to/from the surfaces of PLGA constructs depends on negative charge density of the polymers. For example, the amount of BMP-2 (positively charged growth factor) adsorbed to the surface of porous PLGA MPs was directly related to the negative charge density of the PLGA polymer.[30] Furthermore, "release" (*i.e.* desorption) of BMP-2 was most prolonged through the use of low molecular weight, acid-terminated PLGA, which had the greatest negative charge density.[30] Another recent study showed that therapeutic cationic peptides could be sustainably "released" from the surface of low molecular weight, acid-terminated PLGA MPs and films for more than two weeks.[15] In both of these studies, the PLGA constructs were soaked in solutions of a particular cationic protein or peptide, so sustained "release" was entirely due to prolonged surface desorption resulting from agent–polymer electrostatic interactions. Additionally, these studies investigated the effects of polymer matrix charge density on "release", rather than the influence of the amount of positive charge on the peptide or protein.[15,30]

Accordingly, in the present study, we investigated the influence of peptide charge on release kinetics from a given PLGA formulation. Here, the peptides were encapsulated within PLGA MPs by a common emulsion-solvent evaporation method, instead of being sorbed to the surface of pre-fabricated PLGA constructs. Compared to surface sorption, encapsulation of peptides within PLGA MPs generally enables release for longer periods of time (depending on the polymer), and may better protect peptides from enzymatic degradation *in vivo*.[31,32] Encapsulation, as opposed to surface sorption, also means that release kinetics would be influenced both by erosion of the surrounding polymer matrix and by peptide–polymer electrostatic interactions. Specifically, as a polymer matrix becomes sufficiently porous and diffusion is no longer physically constrained, we hypothesized that release would be hindered by peptide–polymer interactions, in proportion to the positive charge (per mass) of the peptide. Indeed, we observed striking

inverse correlations between net positive charge on a peptide and release rates (following the lag phase) from all polymers, including high molecular weight and ester-capped PLGAs (Fig. 2 and 3). Notably, since peptide release was detected by fluorescence, native peptide and acylated peptide–PLGA adducts in release media are not differentiated (as by HPLC-MS[16]). Therefore, this study does not specifically distinguish between contributions of electrostatic interactions and peptide acylation to slower release kinetics for more positively charged peptides.

Attention to electrostatic or covalent interactions between charged peptides and polymers could also give key insight into new strategies to achieve desired release kinetics. For instance, whereas fast release of uncharged agents would traditionally be achieved with fast degrading, acid-terminated, low molecular weight polymers (as in Fig. 1), such polymers substantially delay release of positively charged agents (as in Fig. 2C and 6B), due to agent–polymer interactions. Therefore, faster release of cationic peptides and proteins might be accomplished instead by using very low molecule weight ester-capped PLGA. Although ester-capped PLGA degrades more slowly than uncapped PLGA of similar molecular weight,[25] it would exhibit less negative charge, and thus reduced interactions with cationic agents. Furthermore, rapid bulk erosion of the polymer matrix, due to the low initial molecular weight, would translate to fewer physical barriers to egress of encapsulated agents. Despite the fact that PLGA has a proven track record with the FDA, and is therefore widely used, alternate biodegradable polymers with neutral or positive charge (*e.g.* polyketals,[33] polyphosphazenes,[34] or poly(β amino esters)[22]) may actually be used to enable faster release of cationic agents, or more sustained release of anionic agents. Finally, co-encapsulation of excipients that would neutralize electrostatic interactions between PLGA and cationic peptides may accelerate release kinetics. For example, inorganic divalent cations (*e.g.* Ca^{2+} or Mn^{2+}) have been shown to reduce adsorption of a cationic peptide on the surface of acid-terminated PLGA, as well as subsequent acylation reactions.[12,18] Alternatively, polyanionic excipients (*e.g.* chondroitin sulfate[35]) that complex with cationic peptides could also reduce peptide–polymer electrostatic interactions and permit faster release by masking the positive charge of the peptide.

While the aforementioned approaches to tune release kinetics involve altering properties of the delivery system, correlations between agent charge and release kinetics could also motivate novel ways to control release by modifying the encapsulated agent itself. Desired release kinetics for a given agent are traditionally attained by selecting a polymer with a particular combination of initial molecular weight, hydrophobicity (end-group chemistry), and lactide to glycolide ratio. Unfortunately, polymers chosen for preferable release rates may not have ideal physical properties for the intended application. Since the amount of positive charge on a peptide influences its rate of release from each polymer (Fig. 2 and 3), chemical modification of therapeutic agents to increase or reduce positive charge could prolong or accelerate release from any polymer chosen for its physical properties. For peptides and proteins, various chemical modifications (acetylation, methylation, PEGylation, aminoalkylation, *etc.*) have been used to increase half-life, or alter bioavailability, bioactivity, and solubility. Addition or deletion of charged amino acids (without altering protein function), or modification of charged residues can eliminate or enhance positive or negative charge (and acylation targets, such as primary amine groups), and the degree of modification can be controlled by reagent stoichiometry.[36] Just as chemical modification of proteins has been used to study effects of protein surface charge on self-assembly with gold nanoparticles,[37] modification of peptides and proteins may also be used to tune release kinetics from a given polymer.

In contrast to invariant net charge of some cationic peptides, net charge of some peptides with low isoelectric points is a function of the pH of the local microenvironment (Fig. 5A). Previous studies have noted inverse relationships between ''acid number'' (a measure of carboxylic acid content of a polymer) and PLGA molecular weight or end-group chemistry.[30,38] Here, we show that initial polymer chemistry also dictates evolution of bulk intraparticle pH during MP degradation (Fig. 4A). Specifically, higher molecular weight (43 kDa) and ester-capped PLGA MPs have higher initial intraparticle pH and more gradual decreases in pH than lower molecular weight uncapped PLGA (Fig. 4A). Importantly, pH within MPs degrading *in vivo* may differ from that measured *in vitro*, due to differences in external volume, buffering capacity of interstitial fluid, and the presence of enzymes that contribute to PLGA degradation *in vivo*. Still, understanding the dynamic intraparticle microclimate enables estimates of peptide charge, which in turn could explain unconventional release kinetics. For example, without peptide–polymer interactions, we would expect faster release and greater initial burst from more hydrophilic uncapped PLGA, due to faster hydration and degradation.[28] Instead, some peptides have greater early release from ester-capped PLGA MPs (Fig. 5 and Fig. S2, ESI†), likely due to higher intraparticle pH and resultant less positive peptide charge. Since acylated peptide adducts form over the course of particle degradation, and not during particle fabrication,[17] initial burst release may not be influenced by peptide acylation; however, faster evolution of more acidic intraparticle pH in some PLGA MPs (Fig. 4) may promote greater acylation and contribute to slower release at later time points, since acylation reactions are catalyzed by acidic pH.[16]

It is worth noting that measurements of bulk intraparticle pH may overestimate acidity near the particle surface, since radial pH gradients exist in MPs.[27,39,40] This could translate into slight overestimates of net charge for pH-dependent peptides (Fig. 5B), especially near the surface of MPs. Microclimate pH near the particle surface is, however, likely still lower than external supernatant pH, since continuous ester hydrolysis generates tethered carboxylic acid groups at the matrix surface faster than associated protons can diffuse away with buffer salt counterions. This is evidenced by the presence of radial pH gradients in well-hydrated matrices, which would be permeable to buffer salts from external media.[27,39,40] Additionally, since peptides are initially sorbed to dry PLGA matrix (before hydration), pre-sorbed peptides may compete with incoming buffer

salts for the protons associated with tethered carboxylic acid groups on the matrix.

Differences in early release from uncapped and ester-capped PLGA MPs (Fig. 5C) could also be attributed in part to competing electrostatic interactions within a single peptide, between multiple peptides, or between a peptide and the PLGA matrix. In a somewhat less acidic microclimate, the pH-dependent peptides would contain both unprotonated acidic residues (negatively charged) and protonated basic residues (positively charged). Negative or neutral net charge (due to more acidic residues) could mask the fact that positively charged residues may interact electrostatically with negatively charged residues from the same or nearby peptides, or with the negatively charged PLGA matrix. In a matrix with less negative charge density (*e.g.* ester-capped PLGA), electrostatic interactions among peptides might dominate, whereas in a matrix with greater negative charge density (*e.g.* uncapped PLGA), electrostatic interactions between peptides and the matrix might be dominant. This competition for electrostatic interactions could contribute to faster release of CK1sub peptide from ester-terminated PLGA, relative to uncapped PLGA (Fig. 5C). In terms of cationic peptides with few acidic residues (*e.g.* +3.1 kDa^{-1} peptide), less intra- and inter-peptide electrostatic interactions may allow peptide–PLGA interactions to dominate, resulting in impeded release even from ester-capped PLGA with less negative charge density (Fig. 2F).

Admittedly, peptide–polymer electrostatic interactions are not the only factor that influences early release kinetics. For example, greater initial burst for peptides with initial negative charge from low molecular weight 7 kDa PLGA MPs and minimal burst of those peptides from 43 kDa PLGA MPs (Fig. 5D) may be attributed to greater matrix permeability of MPs made of the lower molecular weight 7 kDa PLGA. This notion is consistent with a previous report indicating that peptides can penetrate hydrophilic (acid-terminated), low molecular weight PLGA to a much greater extent than higher molecular weight PLGA, which lacks sufficiently mobilized polymer chains.[15] It is also supported by our observation of initial higher intraparticle pH and lower supernatant pH for 7 kDa, relative to 15 kDa, PLGA MPs (Fig. 4), which indicates a substantial number of acidic PLGA polymer chains may able to diffuse out of the 7 kDa PLGA MPs upon hydration. We expect this is due to the lower initial molecular weight PLGA having more polymer chains below the critical molecular weight for water solubility ($\sim$1050 Da[41]).

In the past decade, research (by our lab and others) has focused on controlled delivery of chemokines, cytokines, protein antigens, and growth factors from polymeric MPs and scaffolds, with numerous therapeutic applications.[20,21,31,42–44] Notably, many of these proteins have significant positive charge at varying intraparticle pH (Fig. 6A and Table 2), which could contribute to impeded release from negatively charged polymeric delivery systems. Comparisons of release kinetics for several proteins and oligonucleotides with different net charge profiles (Fig. 6) suggest that, as with smaller peptides, release of larger biomolecules is impacted by electrostatic interactions. Specifically, a high degree of net positive charge on proteins (*e.g.* CCL21 and CCL22) considerably slows their release, even from porous MPs, which have pre-established pathways for release of even large encapsulated agents. In contrast, proteins and oligonucleotides with less positive charge or negative charge tend to release faster from MPs with similar formulation characteristics. Overall, our observations of early release kinetics for peptides and release of larger biomolecules are consistent with anecdotal reports of greater initial burst for proteins with lower isoelectric points (*i.e.* those that could have initial net negative charge within some PLGA MPs). For example, Lee *et al.* noted 20–50 percent initial burst of insulin (pI 5.4), compared to less than 10 percent initial burst for VEGF (pI 8.5), both encapsulated in 10 kDa PLGA MPs.[45] Therefore, we expect examination of protein charge *vs.* pH relationships and prediction of dynamic intraparticle pH will lead to better design of formulations to achieve desired release kinetics for a wide variety of peptide and protein therapeutics, including those in Table 2. Furthermore, agent–polymer charge interactions may have an even greater impact on release of positively charged small molecule drugs, which may have greater charge density (*e.g.* gentamicin +10.5 kDa^{-1}, metformin +15.5 kDa^{-1}, or olanzapine +6.1 kDa^{-1} at pH 3). The small size of these drugs would allow them to diffuse more freely through a given polymer matrix, so considerable positive charge density could have a more striking impact on impeding release. Finally, drug analogs with added positive charge may enable more sustained release of small molecules, for which even very high molecular weight, slow degrading polymers may not serve to sufficiently sustain release.

Table 2 Therapeutic peptides & proteins with positive or variable net charge

Protein/peptide	NCBI/Drug Bank Accession (residues)	M_W (kDa)	pI	Charge per kDa	
				pH 5	pH 3
CXCL10 (IP-10)	P02778 (22–98)	8.6	10.7	+1.38	+1.95
CXCL12 (SDF1α)	P48061 (22–89)	8.0	10.3	+1.42	+1.87
bFGF	P09038 (143–288)	16.4	9.9	+0.88	+1.64
PDGF-BB (dimer)	P01127 (82–190)	24.6	9.3	+0.83	+1.51
TGF-β1 (dimer)	P01137 (279–390)	25.6	8.2	+0.59	+1.13
BMP-2 (dimer)	P12643 (283–396)	25.8	7.9	+0.67	+1.41
IL-12p40	P29460 (23–328)	34.7	5.3	+0.07	+1.13
GM-CSF	P04141 (18–144)	14.5	5.0	−0.00	+0.97
EGF	P01133 (971–1023)	6.2	4.6	−0.20	+1.02
Exenatide	DB01276	4.2	4.5	−0.30	+0.91
Enfuvirtide	DB00109	4.5	4.1	−0.70	+0.62
Thymalfasin	DB04900	3.1	4.0	−1.27	+1.14

Conclusions

We have identified pronounced, inverse correlations between positive net charge on peptides and the rates of release from PLGA MPs. Our empirical measurements of intraparticle pH demonstrate considerable influence of PLGA chemistry, with less acidic microenvironments present in higher molecular weight or ester-capped PLGA MPs. Such information enabled estimates of peptide charge in degrading PLGA MPs, which suggest that initial net charge of certain peptides (with low isoelectric points) may be negative in ester-capped PLGA, but

positive in uncapped PLGA. This could explain the otherwise counterintuitive, faster early release from the slower degrading ester-capped PLGA MPs, relative to faster degrading uncapped PLGA MPs. By demonstrating that our results with model peptides extend to larger biomolecules (proteins and oligonucleotides), we underscore the importance and broad relevance of agent–polymer charge interactions to the field of controlled release. Finally, we expect that these trends between biomolecule charge and release kinetics will improve future design of controlled release formulations for a wide range of therapeutically relevant peptides and proteins, and may be incorporated into mathematical models of controlled release to improve their predictive capacity.

Acknowledgements

We thank the University of Pittsburgh's Center for Biological Imaging for assistance with SEM imaging, and Dan Maskarinec for help with CCL22 MP fabrication and related data collection. This work was supported by the NIH (R01 DE021058-01), the Wallace H. Coulter Foundation, the Camille and Henry Dreyfus Foundation, and the Arnold and Mabel Beckman Foundation (to S.R.L.). S.C.B. is the recipient of an NSF Graduate Research Fellowship (DGE-1247842), and A.J.G. is the recipient of an NIH F31 Award (DE021297-01). A.C.Z. was supported by the University of Pittsburgh's Brackenridge Research Fellowship and Chancellor's Undergraduate Research Fellowship, and J.M.W. was supported by an NSF Research Experience for Undergraduates (REU) program (EEC-1005048).

References

1 BCC Research, Global Markets and Manufacturing Technologies for Protein Drugs, 2013.
2 A. A. Kaspar and J. M. Reichert, *Drug Discovery Today*, 2013, **18**, 807–817.
3 L. Osterberg and T. Blaschke, *N. Engl. J. Med.*, 2005, **353**, 487–497.
4 National Heart Lung and Blood Institute, NHLBI Fact Book, Fiscal Year 2012, Bethesda, MD, 2013.
5 S. N. Rothstein and S. R. Little, *J. Mater. Chem.*, 2011, **21**, 29–39.
6 A. N. Ford Versypt, D. W. Pack and R. D. Braatz, *J. Controlled Release*, 2013, **165**, 29–37.
7 S. N. Rothstein, S. R. Little and W. J. Federspiel, *J. Mater. Chem.*, 2008, **18**, 1873–1880.
8 S. N. Rothstein, W. J. Federspiel and S. R. Little, *Biomaterials*, 2009, **30**, 1657–1664.
9 S. Fredenberg, M. Wahlgren, M. Reslow and A. Axelsson, *Int. J. Pharm.*, 2011, **415**, 34–52.
10 H. K. Makadia and S. J. Siegel, *Polymers*, 2011, **3**, 1377–1397.
11 R. C. Mundargi, V. R. Babu, V. Rangaswamy, P. Patel and T. M. Aminabhavi, *J. Controlled Release*, 2008, **125**, 193–209.
12 A. M. Sophocleous, Y. Zhang and S. P. Schwendeman, *J. Controlled Release*, 2009, **137**, 179–184.
13 M. M. Gaspar, D. Blanco, M. E. Cruz and M. J. Alonso, *J. Controlled Release*, 1998, **52**, 53–62.
14 M. D. Blanco and M. J. Alonso, *Eur. J. Pharm. Biopharm.*, 1997, **43**, 287–294.
15 A. M. Sophocleous, K. G. Desai, J. M. Mazzara, L. Tong, J. X. Cheng, K. F. Olsen and S. P. Schwendeman, *J. Controlled Release*, 2013, **172**, 662–670.
16 A. Lucke, J. Kiermaier and A. Gopferich, *Pharm. Res.*, 2002, **19**, 175–181.
17 A. H. Ghassemi, M. J. van Steenbergen, A. Barendregt, H. Talsma, R. J. Kok, C. F. van Nostrum, D. J. Crommelin and W. E. Hennink, *Pharm. Res.*, 2012, **29**, 110–120.
18 Y. Zhang and S. P. Schwendeman, *J. Controlled Release*, 2012, **162**, 119–126.
19 M. Sen, S. M. Thomas, S. Kim, J. I. Yeh, R. L. Ferris, J. T. Johnson, U. Duvvuri, J. Lee, N. Sahu, S. Joyce, M. L. Freilino, H. Shi, C. Li, D. Ly, S. Rapireddy, J. P. Etter, P. K. Li, L. Wang, S. Chiosea, R. R. Seethala, W. E. Gooding, X. Chen, N. Kaminski, K. Pandit, D. E. Johnson and J. R. Grandis, *Cancer Discovery*, 2012, **2**, 694–705.
20 S. Jhunjhunwala, G. Raimondi, A. J. Glowacki, S. J. Hall, D. Maskarinec, S. H. Thorne, A. W. Thomson and S. R. Little, *Adv. Mater.*, 2012, **24**, 4735–4738.
21 S. Jhunjhunwala, S. C. Balmert, G. Raimondi, E. Dons, E. E. Nichols, A. W. Thomson and S. R. Little, *J. Controlled Release*, 2012, **159**, 78–84.
22 S. R. Little, D. M. Lynn, S. V. Puram and R. Langer, *J. Controlled Release*, 2005, **107**, 449–462.
23 A. Shenderova, T. G. Burke and S. P. Schwendeman, *Pharm. Res.*, 1999, **16**, 241–248.
24 A. L. Lehninger, *Principles of biochemistry*, Worth Publishers, New York, 1982.
25 M. A. Tracy, K. L. Ward, L. Firouzabadian, Y. Wang, N. Dong, R. Qian and Y. Zhang, *Biomaterials*, 1999, **20**, 1057–1062.
26 A. N. Ford Versypt, D. W. Pack and R. D. Braatz, *J. Controlled Release*, 2013, **165**, 29–37.
27 K. Fu, D. W. Pack, A. M. Klibanov and R. Langer, *Pharm. Res.*, 2000, **17**, 100–106.
28 Y. Yeo and K. Park, *Arch. Pharmacal Res.*, 2004, **27**, 1–12.
29 J. Herrmann and R. Bodmeier, *J. Controlled Release*, 1995, **36**, 63–71.
30 J. A. Schrier and P. P. DeLuca, *AAPS PharmSciTech*, 2001, **2**, 66–72.
31 P. Tayalia and D. J. Mooney, *Adv. Mater.*, 2009, **21**, 3269–3285.
32 E. Allemann, J. Leroux and R. Gurny, *Adv. Drug Delivery Rev.*, 1998, **34**, 171–189.
33 S. C. Yang, M. Bhide, I. N. Crispe, R. H. Pierce and N. Murthy, *Bioconjugate Chem.*, 2008, **19**, 1164–1169.
34 H. R. Allcock and N. L. Morozowich, *Polym. Chem.*, 2012, **3**, 578–590.
35 E. S. Lee, K. H. Park, D. Kang, I. S. Park, H. Y. Min, D. H. Lee, S. Kim, J. H. Kim and K. Na, *Biomaterials*, 2007, **28**, 2754–2762.
36 R. L. Lundblad, *Chemical reagents for protein modification*, CRC Press, Boca Raton, 4th edn, 2013.
37 J. A. Jamison, E. L. Bryant, S. B. Kadali, M. S. Wong, V. L. Colvin, K. S. Matthews and M. K. Calabretta, *J. Nanopart. Res.*, 2011, **13**, 625–636.
38 D. H. Na and P. P. DeLuca, *Pharm. Res.*, 2005, **22**, 736–742.
39 Y. Liu and S. P. Schwendeman, *Mol. Pharmaceutics*, 2012, **9**, 1342–1350.

40 Y. Liu, A. H. Ghassemi, W. E. Hennink and S. P. Schwendeman, *Biomaterials*, 2012, **33**, 7584–7593.
41 T. G. Park, *J. Controlled Release*, 1994, **30**, 161–173.
42 A. J. Glowacki, S. Yoshizawa, S. Jhunjhunwala, A. E. Vieira, G. P. Garlet, C. Sfeir and S. R. Little, *Proc. Natl. Acad. Sci. U. S. A.*, 2013, **110**, 18525–18530.
43 Y. Wang and D. J. Irvine, *Biomaterials*, 2011, **32**, 4903–4913.
44 S. N. Rothstein, C. Donahue, L. D. Falo and S. R. Little, *J. Mater. Chem. B*, 2014, **2**, 6183–6187.
45 J. Lee, Y. J. Oh, S. K. Lee and K. Y. Lee, *J. Controlled Release*, 2010, **146**, 61–67.

